Corey, E. J., Katzenellenbogen, J. A., & Posner, G. H. (1967) *J. Am. Chem. Soc. 89*, 4245–4247.
Corey, E. J., Achiwa, K., & Katzenellenbogen, J. A. (1969) *J. Am. Chem. Soc. 91*, 4318–4320.
Cornforth, R. H., & Popják, G. (1969) *Methods Enzymol. 15*, 359–390.
Cramer, F., & Böhm, W. (1959) *Angew. Chem. 71*, 775.
Croteau, R. (1984) in *Isopentenoids in Plants* (Nes, W. D., Fuller, G., & Tsai, L.-S., Eds.) pp 31–64, Marcel Dekker, New York.
Croteau, R. (1985) in *Model Building in Plant Physiology/Biochemistry* (Newman, D. W., & Wilson, K. G., Eds.) CRC Press, Boca Raton FL (in press).
Croteau, R., & Karp, F. (1976) *Arch. Biochem. Biophys. 176*, 734–746.
Croteau, R., & Karp, F. (1977a) *Arch. Biochem. Biophys. 179*, 257–265.
Croteau, R., & Karp, F. (1977b) *Arch. Biochem. Biophys. 184*, 77–86.
Croteau, R., & Karp, F. (1979a) *Arch. Biochem. Biophys. 198*, 512–522.
Croteau, R., & Karp, F. (1979b) *Arch. Biochem. Biophys. 198*, 523–532.
Croteau, R., & Cane, D. E. (1985) *Methods Enzymol. 110*, 383–405.
Croteau, R., & Shaskus, J. (1985) *Arch. Biochem. Biophys. 236*, 535–543.
Croteau, R., Shaskus, J., Cane, D. E., Saito, A., & Chang, C. (1984) *J. Am. Chem. Soc. 106*, 1142–1143.
Croteau, R., Felton, N. M., & Wheeler, C. J. (1985) *J. Biol. Chem. 260*, 5956–5962.
Del Campo, G., Puente, J., Valenzuela, M. A., Traverso-Cori, A., & Cori, O. (1977) *Biochem. J. 167*, 525–529.
Dugan, R. E., Rasson, E., & Porter, J. W. (1968) *Anal. Biochem. 22*, 249–259.
Fernley, H. N. (1971) *Enzymes (3rd Ed.) 4*, 417–447.
Gotfredsen, S., Obrecht, J. P., & Arigoni, D. (1977) *Chimia 31*, 62–63.
Hollander, V. P. (1971) *Enzymes (3rd Ed.) 4*, 449–498.
Hutchinson, C. R., & Makune, C. T. (1976) *J. Labelled Compd. Radiopharm. 8*, 571–574.
Jacobson, H. I., Griffin, M. J., & Jensen, E. V. (1957) *J. Am. Chem. Soc. 79*, 2608–2612.
Kornberg, A., & Pricer, W. E., Jr. (1951) *J. Biol. Chem. 191*, 535–541.
Loomis, W. D., Lile, J. D., Sandstrom, R. P., & Burbott, A. J. (1979) *Phytochemistry 18*, 1049–1054.
Mash, E. A., Gurria, G. M., & Poulter, C. D. (1981) *J. Am. Chem. Soc. 103*, 3927–3929.
McCormick, J. P., & Barton, D. L. (1978) *Tetrahedron 34*, 325–330.
Michelson, A. M. (1964) *Biochim. Biophys. Acta 91*, 1–13.
Poulter, C. D., & King, C.-H. R. (1982a) *J. Am. Chem. Soc. 104*, 1420–1422.
Poulter, C. D., & King, C.-H. R. (1982b) *J. Am. Chem. Soc. 104*, 1422–1424.
Rose, I. A. (1979) *Adv. Enzymol. Relat. Areas Mol. Biol. 50*, 361–395.
Saito, A., & Rilling, H. C. (1979) *J. Biol. Chem. 254*, 8511–8515.
Still, W. C., Kahn, M., & Mitra, A. (1978) *J. Org. Chem. 43*, 2923–2925.
Tidd, B. K. (1971) *J. Chem. Soc. B*, 1168–1176.
Upper, C. D., & West, C. A. (1967) *J. Biol. Chem. 252*, 3285–3292.

Interaction of Adriamycin with Negatively Charged Model Membranes: Evidence of Two Types of Binding Sites†

Nelly Henry, Elzi O. Fantine,‡ Jacques Bolard,* and Arlette Garnier-Suillerot*

Département de Recherches Physiques (UA CNRS 71), Université Pierre et Marie Curie, 75230 Paris Cedex 05, France, and Laboratoire de Chimie Bioinorganique (UA CNRS 71), U.E.R. de Santé, Médecine et Biologie Humaine, Université Paris-Nord, 93012 Bobigny Cedex, France

Received May 7, 1985

ABSTRACT: The interaction of the antitumor compound adriamycin with negatively charged unilamellar phospholipid vesicles was studied. The negative charges were provided by cardiolipin or phosphatidic acid. By analyzing the changes in the circular dichroism spectrum of adriamycin, we demonstrated the presence of two different spectral patterns corresponding to two different binding sites (I and II) on the vesicles. In site I, the amino sugar of adriamycin is bound to the ionized phosphate of either cardiolipin or phosphatidic acid, and the dihydroxyanthraquinone lies outside the bilayer. In site II, the amino sugar is still bound to the phosphate, but the dihydroxyanthraquinone moiety is embedded in the bilayer. This has been shown by measuring spectroscopically the binding of the aglycon part to an external probe and by measuring the susceptibility of bound adriamycin to reduction by NADH dehydrogenase.

The anthracycline antibiotic adriamycin (Adr) is an important antitumor agent with marked activity against a wide variety of human neoplasms (Blum & Carter, 1974; Lenaz & Page, 1976). From studies on the mechanism of action of anthracyclines in vivo, nuclear DNA has usually been considered the prime target for this antibiotic's antineoplastic action (Di Marco, 1975). However, recent studies have suggested that anthracyclines may be cytotoxic primarily as a result of mechanisms other than DNA binding (Duvernay et al., 1980): anthracyclines having a low affinity for DNA are still capable of inhibiting cell mitosis (Israel et al., 1975), and

† This work was supported, in part, by an Association pour la Recherche sur le Cancer (ARC) grant.
* Address correspondence to these authors at Université Paris-Nord.
‡ Present address: Departamento de Quimica, Universidonde Federal de Minas Gerois, Belo Horizonte, Brazil.

0006-2960/85/0424-7085$01.50/0 © 1985 American Chemical Society

Tritton & Yee (1982) have shown that Adr exerts a cytotoxic effect on L 1210 cells without entering them.

Adr interacts both with cell plasma membranes [for a review, see Goormatigh & Ruysschaert (1984)] and with membranes of intracellular components. Both types of interaction play a role in its antibiotic activity. First, the concentration of the drug at the intracellular target is determined by the rates of drug entry and exit from the cells, i.e., its membrane transport (Skovsgaard & Nissen, 1982). Second, Adr is cardiotoxic (Ferrans, 1978); the impairment of mitochondrial function (Doroshow, 1981; Thayer, 1977), possibly resulting from specific Adr–cardiolipin binding (Duarte-Karim et al., 1976; Tritton et al., 1978), is thought to be the primary cause of its cardiotoxicity.

Therefore, several studies have been devoted to the interaction of Adr with phospholipid vesicles in order to determine the thermodynamic and structural parameters of the drug's interaction with specific lipid components. The results obtained also afforded information for a better handling of liposomes as Adr carriers (Forssen & Tökés, 1979, 1981; Gabizon et al., 1982; Rahman et al., 1984).

It appeared that Adr binds more strongly to cardiolipin, which bears two negative charges, than to neutral phospholipids. However, some discrepancies existed between the different studies as, for instance, the location of the aglycon part, the stoichiometry of the binding, whether or not the drug binds to neutral lipids, and the differences in binding to various negatively charged lipids. In the present paper, the interaction of the drug with large and small unilamellar vesicles (LUV and SUV, respectively) is studied, taking advantage of the high sensitivity of circular dichroism (CD) to detect changes in the conformation and the self-association of Adr molecules. Embedding of the drug in the lipid bilayers was further ascertained by measuring the binding of the aglycon part to an external probe and by measuring the amount of Adr susceptible to reduction by NADH dehydrogenase.

From data obtained by these complementary methods, we inferred the presence of two types of binding sites for Adr. In both, the amino sugar is bound to the ionized phosphate of either cardiolipin or phosphatidic acid. In site I, the dihydroanthraquinone moiety lies outside the bilayer, whereas in site II this moiety is embedded in the bilayer.

Materials and Methods

Purified adriamycin (Adr) was kindly provided by Laboratoires Roger Bellon (France). Concentrations were determined by diluting aqueous stock solutions to approximately 10^{-5} M and using $\epsilon_{480} = 11\,500\ M^{-1}\ cm^{-1}$ (Chaires et al., 1982). As anthracycline solutions are sensitive to light and oxygen, stock solutions were prepared just before use. Cytochrome *c* (type VI from horse heart), NADH (grade III), cardiac NADH dehydrogenase, L-α-dipalmitoylphosphatidylcholine (DPPC), L-α-phosphatidylcholine (EPC) from egg yolk type V-E, cardiolipin (CL) from beef heart, egg phosphatidic acid (EPA), and egg phosphatidylglycerol (EPG) were purchased from Sigma Chemical Co., and superoxide dismutase (SOD) was from Behring. All other reagents were of the highest quality available, and deionized, double-distilled water was used throughout the experiments. Unless stated otherwise, buffer solutions were 0.01 M Hepes [*N*-(2-hydroxyethyl)-piperazine-*N*'-2-ethanesulfonic acid] and 0.1 M KCl, pH 7.4. 5(6)-Carboxyfluorescein (CF) was obtained from Kodak Laboratory Chemicals and purified according to Ralston et al. (1981).

Absorption spectra were recorded on a Cary 219 spectrophotometer and circular dichroism spectra on a Jobin Yvon Mark V dichrograph. In the figures $\Delta\epsilon$ is the differential molar dichroic absorption coefficient (10^3 cm^2/mol). The spectra of the suspensions of vesicles without antibiotic were subtracted from those with antibiotic. They consisted of a plain curve of increasing $\Delta\epsilon$ with decreasing wavelength, originating from the light scattering of vesicles. This light scattering is not expected to perturb the CD spectra of the antibiotics embedded in the bilayers of the vesicles because the size parameters (X) of the LUV and SUV are respectively 1.25 and 0.2 ($X = 2\pi a/\lambda$ where a is the radius of the sphere and λ the wavelength, here 400 nm). Under these conditions, the CD spectrum for spheres is similar to the intrinsic CD spectrum (Bohren, 1976).

Unilamellar Phospholipid Vesicles. SUV were prepared according to Newman & Huang (1975). Sonication was performed above the transition temperature of the phospholipids and under nitrogen. LUV were obtained by the phase reversion method (Szoka et al., 1980).

All the experiments were carried out at 22 °C. Under these conditions, DPPC vesicles were in the gel state and EPC vesicles in the liquid-crystalline state.

NADH Dehydrogenase Assay. NADH dehydrogenase activity was determined at 25 °C by modification of a method described previously (Malher, 1955) using cytochrome *c* as the electron acceptor. Adr, in the presence of various amounts of EPA- or EPC-containing vesicles, was assayed for its NADH–cytochrome *c* reductase activity by following cytochrome *c* reduction at 550 nm. The difference between the extinction coefficient of reduced and oxidized cytochrome *c* was taken to equal $19\,600\ M^{-1}\ cm^{-1}$. Unless otherwise stated, the reaction mixture contained Hepes buffer (0.05 M, pH 7.2), 150 μM cytochrome *c*, 77 μM NADH, 18 units/L NADH dehydrogenase, 60 μM Adr, and EPA-containing vesicles. The molar ratio of EPA to Adr ranged from 0:1 to 4:1. The reaction was initiated by the addition of the enzyme. Enzymatic activity is expressed in units, such that 1 unit is the amount of enzyme that reduces 1 μmol of cytochrome *c* per minute at pH 7.2 and 25 °C under the reaction conditions specified above. The production of superoxide anion in the experimental samples was calculated from the rate of cytochrome *c* reduction inhibited by SOD (20 μg/mL).

The rate of oxygen consumption was determined at 25 °C with a YSI 5331 oxygen monitoring system under the reaction conditions outlined above but without cytochrome *c*. The reaction was initiated by the addition of NADH to the reaction chamber through the access slot of the oxygen electrode plunger. The rate of oxygen consumption was calculated from a value of 256 μM for the total dissolved oxygen content of the reaction mixture.

Results

Circular Dichroism Studies. (A) Interaction of Adr with EPA-Containing LUV. As has already been reported, the CD spectrum of adriamycin is largely dependent on the association state of the drug (Martin, 1980; Barthelémy-Clavey et al., 1974; Beraldo et al., 1983). At pH 7.4 and 10^{-5} M, Adr is fully in the monomeric form, and the visible CD spectrum consists of one positive band at 465 nm. When the concentration is increased, this band splits into a doublet characteristic of the associated dimeric form, with a positive band at 460 nm and a negative one at 530 nm. The amplitude of the negative band is indicative of the number of molecules in the dimeric form. The CD spectrum was recorded at different concentrations. Using the variation of $\Delta\epsilon$ at 530 nm as a function of the concentration, a constant of dimerization was calculated for 0.1 M ionic strength. The value obtained, K_d

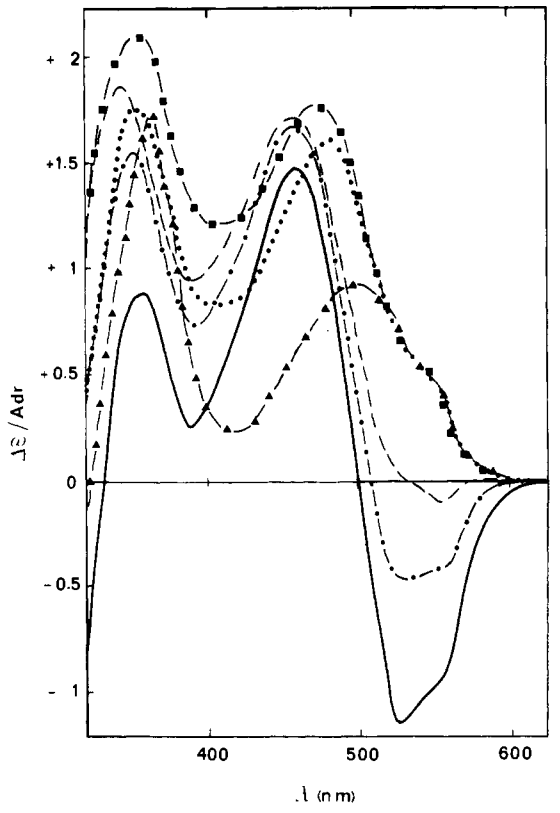

FIGURE 1: Circular dichroism spectra of adriamycin in the presence of EPA-containing LUV. Experimental conditions: 350 μM Adr, Hepes buffer, pH 7.4, I = 0.1. The LUV were prepared with EPC, EPA, and cholesterol in the molar ratio 7:1:2. The molar ratio of EPA to Adr was 0 (—), 0.14 (-·-), 0.28 (--), 0.59 (-■-), 0.83 (···), and 1.7 (-▲-).

= 1.1 × 10^4, compares well with those reported by Martin (1980).

In the following experiments, concentrations of Adr ranging from 2 × 10^{-4} to 4 × 10^{-4} M were used: at these concentrations, the percentage of dimer varied from 60% to 80%. Figure 1 shows the CD spectrum of 3.5 × 10^{-4} M Adr in the presence of increasing amounts of EPA-containing LUV. The LUV were prepared with EPC, EPA, and cholesterol in the molar ratio 7:1:2, but the results were independent of the presence of cholesterol. When the molar ratio of EPA to Adr was varied from 0 to 2, two differential spectral patterns were obtained. As can be seen in Figure 1, when the molar ratio of EPA to Adr was increased from 0 to about 0.5, the CD spectrum changed from that typical of Adr in the dimeric form to another one (hereafter labeled I) which exhibited a positive band at 470 nm and a shoulder at 530 nm. A further increase of the molar ratio of EPA to Adr gave rise to a shift of this band from 470 to 500 nm and to a decrease of its amplitude. This CD pattern will hereafter be labeled II. These two CD patterns strongly suggest the existence of two different types of binding sites of Adr to EPA-containing LUV. The variations of Δε at 530 and 470 nm as a function of the EPA to Adr molar ratio were used to monitor the fixation of Adr to sites I and II, respectively (Figure 2).

The observation that the CD band of Adr bound to site II lay at a higher wavelength than that corresponding to site I strongly suggested that site II is less polar than site I. It should be pointed out that the binding of Adr to these two sites was completed within the 10 s following the mixture. No further changes were observed during the next 48 h.

(*B*) *Interaction of Adr with Cardiolipin-Containing LUV.* Similar results were obtained for the same kind of experiments

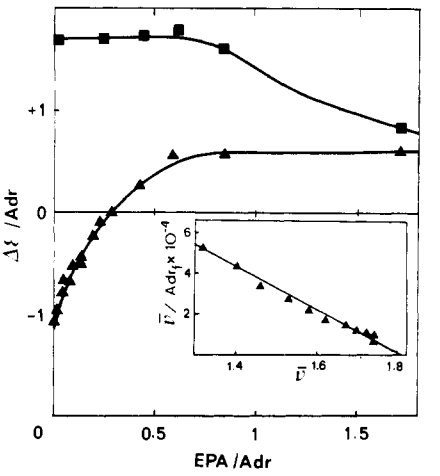

FIGURE 2: Circular dichroism spectra of adriamycin in the presence of EPA-containing LUV. Δε values at 530 (▲) and 470 nm (■) are plotted as a function of the molar ratio of EPA to adriamycin. Experimental conditions: 350 μM Adr, Hepes buffer, pH 7.4, I = 0.1. The LUV were prepared with EPC, EPA, and cholesterol in the molar ratio 7:1:2, t = 22 °C. Insert: Scatchard plot analysis of the binding data of Adr to EPA-containing LUV. $\bar{\nu}$ is Adr bound per EPA, and Adr_f stands for the free Adr concentration.

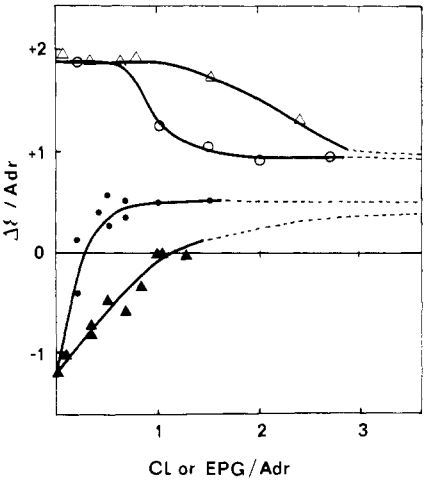

FIGURE 3: Circular dichroism spectra of adriamycin in the presence of CL- or EPG-containing LUV. Δε values at 530 (▲, ●) and 470 nm (△, ○) have been plotted as a function of the molar ratio of CL to Adr (●, ○) or EPG to Adr (▲, △). Experimental conditions: 350 μM Adr, Hepes buffer, pH 7.4, I = 0.1. The LUV were prepared with EPC, CL or EPG, and cholesterol in the molar ratio 7:1:2, t = 22 °C.

performed with CL-containing LUV; i.e., depending on the molar ratio of CL to Adr, two different spectral patterns, characteristic of two different types of binding site, were obtained. The variations of Δε at 530 and 470 nm as a function of the molar ratio of CL to Adr are plotted in Figure 3.

(*C*) *Interaction of Adr with EPG-Containing LUV.* Here again, two different CD spectral patterns were obtained when increasing amounts of EPG-containing LUV were added to Adr. At variance with the two above-described systems, the two types of binding were obtained at higher molar ratios of EPG to Adr. This can be seen in Figure 3 where Δε values at 530 and 470 nm are plotted as a function of the molar ratio of EPG to Adr.

(*D*) *Interaction of Adr with SUV.* Strictly similar results were obtained with EPA-, CL-, or EPG-containing SUV, indicating that the surface curvature did not affect results.

When the same experiments were performed in the absence of EPA (or CL or EPG), the CD spectral pattern corresponding to site I was not observed. Nevertheless, some

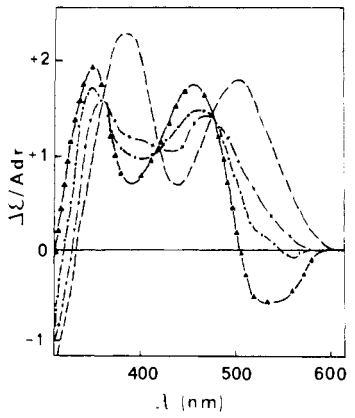

FIGURE 4: CD spectra of the DNA–Adr system as a function of DNA concentration. Experimental conditions: 100 μM Adr, Hepes buffer, pH, 7.4, I = 0.1. The molar ratio of nucleotide to Adr was 0 (–▲–), 1.3 (–·–), 2.6 (–+–), and 50 (––).

modifications of the CD spectrum were observed: a simultaneous decrease of the amplitude of the bands at 528 and 460 nm. This decrease was rather smooth, and the plots of $\Delta\epsilon$ at 528 and 460 nm as a function of the molar ratio of EPC to Adr did not attain a plateau even at molar ratios higher than 20. These modifications were taken as an indication that Adr interacts with EPC; this binding site was labeled III. Furthermore, with DPPC–SUV, that is, SUV in the gel state, we observed that the bands at 528 and 460 nm also decreased but this decrease was smaller.

(*E*) *Comparison of the Adr–LUV System with the Adr–DNA System.* It is worthwhile to compare the negatively charged LUV–Adr system with the previously reported DNA–Adr system. At least two types of binding occur between these drugs and DNA. In one type, the drug molecule intercalates between the base pairs of DNA with the ammonium group of the sugar moiety involved in an electrostatic and H-bonding interaction with a neighboring phosphate group (Gabbay et al., 1976). This occurs at a "high" nucleotide to drug molar ratio, i.e., higher than 6. The other type of binding appears at "low" nucleotide to drug molar ratios once the primary intercalative binding sites have been saturated; the molecule of drug binds to DNA by electrostatic interactions involving the DNA phosphate group and the amino sugar of the drug (Zunino et al., 1972; Goodman et al., 1977). The intercalated binding site of Adr to DNA has been characterized by its CD spectral pattern (Gabbay et al., 1976). Similarly, we characterized the nonintercalated binding sites. Figure 4 shows the CD spectra of 10^{-4} M Adr in the presence of increasing amounts of DNA. At this concentration, in the absence of DNA, about 50% of Adr is in dimeric form. The addition of DNA to give a molar ratio of nucleotide to Adr equal to 1 resulted in the disappearance of the negative band at 530 nm; the CD spectrum, in the visible range, exhibited only a positive band at 460 nm which corresponded to the nonintercalated binding site. A further increase of the nucleotide to Adr molar ratio gave rise to a shift of this band to 510 nm, characteristic of the intercalated site (Gabbay et al., 1976). Thus, in both systems, two CD spectral patterns characteristic of two different types of binding sites of Adr were observed. The CD spectrum of the first type obtained at low EPA (or CL or EPC) to Adr or nucleotide to Adr molar ratios exhibited a positive band at 470 nm while the CD spectrum of the second type obtained at high EPA (or CL or EPG) to Adr or nucleotide to Adr molar ratios exhibited a positive band at 510 nm. These data strongly suggest that in both cases binding of Adr to the macromolecules was similar.

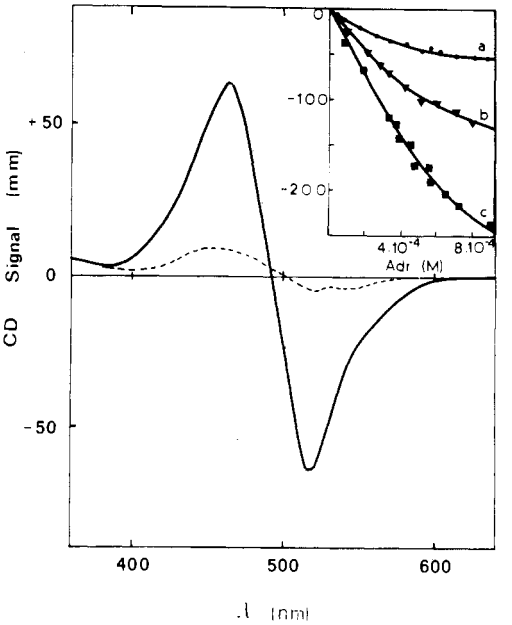

FIGURE 5: Circular dichroism spectra of the Adr–CF complex. Experimental conditions: 2×10^{-4} M Adr in the absence (---) and in the presence of 4×10^{-4} M CF (—), Hepes buffer, pH 7.4, I = 0.1, cell path length e = 0.1 cm, $\sigma = 2 \times 10^{-6}$ (sensitivity of dichrograph). Insert: The amplitude of the CD signal at 518 nm is plotted as a function of the concentration of Adr; the concentration of CF was kept constant and equal to 0.5×10^{-4} (●), 2×10^{-4} (▼), and 4×10^{-4} M (■).

Thus, binding site I of Adr to negatively charged LUV can be accounted for by an electrostatic interaction between the amino sugar moiety of Adr and the charged phosphate group of EPA (or CL or EPG), the dihydroanthraquinone lying outside the bilayer. Binding site II should involve in addition an embedding of the dihydroanthraquinone in the phospholipid bilayer similar to the intercalation between base pairs of DNA.

Additional evidence of these two types of binding sites of Adr to negatively charged SUV or LUV is provided by the following experiments.

Method of Competing Equilibria Using 5(6)-Carboxyfluorescein. CF has been largely used for following liposome–cell (Leserman et al., 1980), cell–cell (Dahl et al., 1981), and liposome–liposome (Wilschut & Papahadjopoulos, 1979) interactions. CF does not interact with the cell membrane but remains in the aqueous media. Furthermore, CF, as shown below, interacts with Adr by forming a complex with a strong CD signal in the visible range. Because of these two properties, CF could be used as a probe to evaluate the accessibility of Adr bound to membranes. CF was thus expected to discriminate molecules bound to the hydrophilic surface from those in the hydrophobic interior of a membrane.

We first determined the physicochemical characteristics of the complex formed between CF and Adr and then used CF as a competing ligand to Adr bound to negatively charged SUV or LUV.

(*A*) *5(6)-Carboxyfluorescein–Adriamycin Interaction in Water: Circular Dichroism Study.* CF in aqueous solution at pH 7.4 absorbs strongly in the visible region with a maximum at 492 nm (ϵ = 60 000 M^{-1} cm^{-1}) (Ralston et al., 1981). Since the molecule is achiral, no circular dichroism was observed even at concentrations where self-association occurs. However, when CF was added to Adr, an intense dichroic doublet centered at 494 nm was observed (Figure 5). Increasing amounts of Adr were added to a constant concentration of CF. In the Figure 5 insert, the amplitude of the CD signal at 518 nm is plotted as a function of the concen-

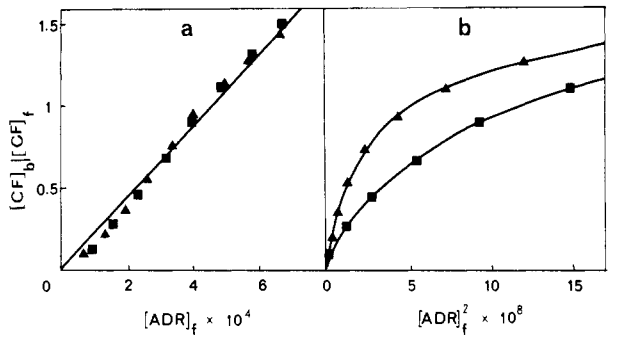

FIGURE 6: Determination of the stoichiometry of the Adr–CF complex. The molar ratio $[CF]_b/[CF]_f$ has been plotted as a function of $[Adr]_f$ (curve a) and $[Adr]_f^2$ (curve b). The experimental conditions are the same as those in Figure 5.

tration of Adr. At a constant concentration of CF equal to 0.5×10^{-4} M, the curve reached a plateau (Figure 5, curve a). $\Delta\epsilon$ per CF is then equal to -23 ± 3 M^{-1} cm^{-1}. This was taken to indicate that CF was totally bound to Adr. Using this value of $\Delta\epsilon$, it is thus possible to calculate in any mixture of Adr and CF the proportions of bound and free CF.

To determine the stoichiometry of the CF–Adr complex, a Job ratio plot (Job, 1936) was constructed by using the $\Delta\epsilon$ at 518 nm to monitor complex formation. The Job plot obtained was rather flat and inaccurate, and it was difficult to decide whether the stoichiometry of CF to Adr was 1:1 or 1:2.

The formation constant (K) is defined by the following equilibrium:

$$CF + n\text{Adr} \rightleftharpoons^{K} CF(\text{Adr})_n$$

with

$$K = [CF(\text{Adr})_n]/[CF]_f[\text{Adr}]_f^n$$

where $[CF]_f$ and $[Adr]_f$ stand for the concentration of free CF and free Adr, respectively, and $[CF(Adr)_n]$ is the concentration of complex, equal to the concentration of bound CF, i.e., $[CF]_b$. Thus

$$K = [CF]_b/[CF]_f[\text{Adr}]_f^n$$

The plot of $[CF]_b/[CF]_f$ as a function of $[Adr]_f^n$ might yield a straight line with a slope equal to K. As it was not possible to decide between a stoichiometry of 1:1 or 1:2 on the basis of the Job plot, we plotted the molar ratio $[CF]_b/[CF]_f$ as a function of $[Adr]_f$ (Figure 6, curve a) and as a function of $[Adr]_f^2$ (Figure 6, curve b). Only the first plot gave a straight line, indicating that the stoichiometry of the complex is 1:1 with a stability constant equal to $(2 \pm 0.5) \times 10^3$.

(B) Interaction of the CF–Adr Complex with Negatively Charged Phospholipid Vesicles. In this section, CF was used as a competing ligand to Adr bound to negatively charged LUV. Increasing amounts of EPA-containing LUV were added to a solution containing 2×10^{-4} M Adr and 4×10^{-4} M CF at pH 7.4. A decrease of the intensity of the dichroic doublet of the Adr–CF complex was observed, and the CD signal at 518 nm was plotted as a function of the molar ratio of EPA to Adr (Figure 7, curve a). Using these data, we calculated $[CF]_b$ and $[CF]_f$. The total concentration of Adr is

$$[\text{Adr}]_T = [\text{Adr}]_{II} + [\text{Adr}]_I + [\text{Adr}]_s + [\text{Adr–CF}]$$

where $[Adr]_{II}$ stands for the concentration of Adr bound to site II, i.e., embedded in the bilayer, $[Adr]_I$ stands for the concentration of Adr bound to the external site I, and $[Adr]_s$

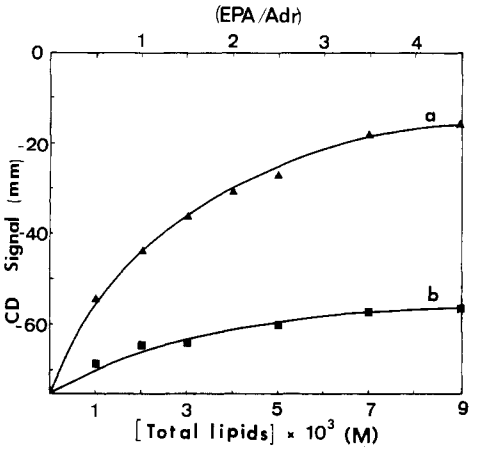

FIGURE 7: Variation at 518 nm of the CD signal of the Adr–CF complex in the presence of increasing amounts of vesicles. Experimental conditions: 2×10^{-4} M Adr, 4×10^{-4} M CF, Hepes buffer, pH 7.4, $I = 0.1$, cell path length $e = 0.1$ cm, $\sigma = 2 \times 10^{-4}$ (sensitivity of the dichrograph). The vesicles were pure lecithin SUV (curve b) and EPA-containing LUV (EPC–EPA–cholesterol in a molar ratio of 7:1:2) (curve a).

stands for the concentration of Adr free in the solution either as a dimer or as a monomer. From the plot of Figure 6, curve a (i.e., $[CF]_b/[CF]_f$ as a function of free [Adr], free [Adr], which is equal to $[Adr]_I + [Adr]_s$, was calculated. It was then possible to calculate $[Adr]_{II}$. In addition, taking into account that the molar ratio of EPA to Adr used ranged from 0.8 to 5.6, we stated that $[Adr]_s$ is negligible in comparison to $[Adr]_{II}$. $[Adr]_{II}$ and $[Adr]_I$ could then be calculated.

Analogous results were obtained with CL-containing LUV. All these results were not time dependent for periods from 10 s to 48 h and did not depend on the order of addition of the components of the mixture. The surface curvature of the vesicles also did not influence the results, since the same results were obtained by using either SUV or LUV.

The ionic strength had a strong effect on the decrease of the CD signal of the Adr–CF complex in the presence of vesicles: the smaller the ionic strength, the greater the decrease. We have previously seen that the ionic strength does not influence complex formation between Adr and CF.

(C) Interaction of the CF–Adr Complex with Neutral Lipid Vesicles. The addition of increasing amounts of neutral lipid vesicles to the Adr–CF complex under the conditions described above gave rise to a less steep decrease of the CD signal (Figure 7, curbe b) than the addition of negatively charged vesicles.

Reduction of Adr by NADH Dehydrogenase in the Presence of SUV. It is well documented that a component of mitochondrial NADH dehydrogenase actively reduces Adr to semiquinone, initiating a free radical cascade (Davies et al., 1983). This reaction can be monitored by following the rate of oxygen consumption. In the presence of NADH (77 μM) and NADH dehydrogenase (18 units/L), increasing concentrations of Adr (up to about 80 μM) gave rise to a linear increase of the rate of oxygen consumption (Fiallo & Garnier-Suillerot, 1985). In the following experiments, Adr was thus used at a concentration lower than 80 μM so that the rate of oxygen consumption would be proportional to the quantity of Adr that could be reduced by the enzyme.

Adr-induced oxygen consumption was measured in the presence of various amounts of EPA-containing vesicles. Figure 8 shows the plot of the rate of oxygen consumption as a function of the molar ratio of EPA to Adr. In this experiment, the concentration of Adr was kept constant at 60 μM.

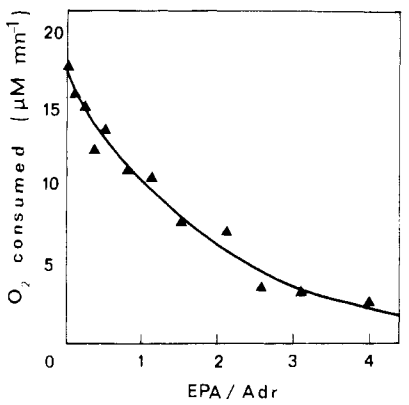

FIGURE 8: Effect of EPA-containing SUV on oxygen consumption by NADH dehydrogenase in the presence of Adr (60 μM). The reaction mixture contained Hepes buffer (0.05 M), pH 7.2, NADH (75 μM), NADH dehydrogenase (18 units/L), and the indicated amount of EPA-containing SUV (EPC–EPA–cholesterol in a molar ratio of 7:1:2).

As shown, the rate of oxygen consumption decreased as the molar ratio of EPA to Adr increased. To check the modifications, if any, of the NADH, NADH dehydrogenase system that could be due to EPA-containing SUV, the rate of reduction of cytochrome *c* was measured (in the absence of Adr) in the presence of increasing concentrations of EPA-containing SUV. No modification of the rate could be detected. These data indicate that through interaction with EPA-containing SUV, Adr loses its ability to transfer electrons from NADH to molecular oxygen; i.e., Adr cannot be further reduced by the enzyme. This has likewise been observed in the presence of cardiolipin-containing SUV (Fiallo & Garnier-Suillerot, 1985). The interpretation given, that insertion of the dihydroanthraquinone moiety in the phospholipid bilayer renders it inaccessible to the enzyme, also holds for Adr in the presence of EPA-containing SUV.

DISCUSSION

The data reported above indicate that two types of binding occur between Adr and the membrane of negatively charged vesicles: type I in which electrostatic interactions occur between the negatively charged phosphate and the positively charged amino group of the sugar moiety of Adr, and type II in which the dihydroanthraquinone moiety is, in addition, embedded in the phospholipid bilayer. Thus, in the presence of negatively charged vesicles, four different forms of Adr can be detected: Adr bound to LUV through either type I or type II and Adr free in the solution either as a dimer (D) or as a monomer (M). As we have demonstrated, CD spectra can be used to distinguish these four forms since each of them exhibits a distinct CD pattern. The two so-called indirect methods can only identify form II, since forms I, M, and D react in the same way to complex formation by CF and reduction by NADH dehydrogenase.

CD measurements of Adr binding appeared to present some advantages over fluorescence measurements (Goldman et al., 1978). In the fluorescence studies, the ratios of two peaks, varying between 1.3 and 1.5, were compared. This variation is small and may be affected by the light scattering of the vesicles; in the circular dichroism studies, the CD spectrum of adriamycin at 528 nm may totally disappear, which allows the interaction to be more easily monitored.

CD data yielded quantitative information for binding site I of Adr. As seen in Figure 1, the value of $\Delta\epsilon$ at 530 nm is the same (+0.6) for Adr bound as type I or as type II. At the same wavelength, the values of $\Delta\epsilon$ are +0.2 and −1.3 for free Adr in the monomeric and the dimeric form, respectively. Thus, taking into account the equilibrium of dimerization of free Adr ($K_d = 1.2 \times 10^4$) and the data of Figure 2, the concentrations of bound Adr (I plus II) and free Adr (M plus D) as a function of the EPA to Adr molar ratio were calculated. The binding data were analyzed by Scatchard plots. Since two different binding sites are involved, the plot should exhibit two slopes. In fact, only one slope is observed (Figure 2, insert). This can easily be explained by the fact that the plot was drawn at a molar ratio of EPA to Adr ranging from 0.1 to 0.7, where binding site II, which is clearly the stronger, is saturated. The slope gives the stability constant for binding site I, $K_I = 10^5$, and the intercept $n_I + n_{II} = 1.8$, where n_I and n_{II} are the number of Adr molecules bound per EPA in site I and site II, respectively.

Scatchard plots were also drawn for Adr with CL- or EPG-containing LUV. In the case of CL, $n_I + n_{II} \simeq 2$ and $K_I \simeq 4 \times 10^4$, and in the case of EPG, $n_I + n_{II} \simeq 0.85$ and $K_I \simeq 3 \times 10^4$. Quantitative information concerning binding site II of Adr was obtained by two indirect methods. At the molar ratios of EPA to Adr used (ranging from 1 to 6), we stated that the concentration of free Adr was negligible compared to that of bound Adr.

The concentrations of embedded (type II) and nonembedded Adr were determined from the rate of oxygen consumption of the Adr–NADH–NADH dehydrogenase system keeping in mind that the rate is maximum when Adr is either free or bound in site I and becomes zero when Adr is bound in site II. The binding data (Figure 8) analyzed by Scatchard plots gave an apparent equilibrium constant of $K_{em} = 3.4 \times 10^4$ and $n_{II} = 0.33$.

As we stated above, the concentration of embedded Adr can also be calculated by the method of competing equilibria using CF. Taking into account the equilibrium constant of the CF–Adr complex previously determined and the data of Figure 6, we determined the concentration of Adr bound in site I and in site II; the Scatchard plot gave an apparent equilibrium constant of $K_{em} = 5.3 \times 10^4$ and $n_{II} = 0.35$.

From these two experiments, a mean value of 4×10^4 was taken for the apparent equilibrium constant of embedding of the dihydroanthraquinone moiety, $n_{II} = 0.34$. Thus, the following values can be adopted: $K_I = 10^5$ and $n_I = 1.5$; $K_{II} = K_I K_{em} = 4 \times 10^9$ and $n_{II} = 0.34$. These values were calculated by using the total concentration of negative charges. It was important next to determine the concentration of EPA or more generally, of negatively charged phospholipid lying in the external leaflet of the membrane.

The number of charges depends on the state of ionization of the vesicle phospholipids. This state is especially sensitive to ionic strength and surface charge (Ptak et al., 1980): a positive charge decreases the pK_a value whereas a negative one increases it, with a total range of variation of 2.5–3 units. At pH 7.4, these effects do not modify the number of charges carried by cardiolipin, that is, two negative charges, because its pK_a is 4. This is not true for phosphatidic acid, for which the two pK_a values were found to be 4 and 8 in pure phosphatidic acid vesicles at 0.1 M ionic strength (Abramson et al., 1964). In the vesicles that we used, the surface potential was less negative, since 80% of the total phospholipids were neutral (cholesterol and phosphatidylcholine). Furthermore, the positive charges of Adr may decrease the negative potential. We can assume that under these conditions the pK_a of phosphatidic acid is lower than 8 and that phosphatidic acid is doubly ionized at pH 7.4. This would explain why we found no significant difference between CL- and EPA-containing

vesicles in their interactions with Adr.

We also have to know the distribution of the negative charges between the external and the internal leaflet of the bilayers. With EPA-containing SUV, it has been shown that all the negative phospholipid molecules are on the external leaflet (Abramson et al., 1964). With EPG, 90% of these molecules are on the external leaflet (Lenz et al., 1982). In our particular cases, we determined this distribution using Massari's method (Massari et al., 1978) and found that with SUV and LUV containing 10% phosphatidic acid or 20% cardiolipin, 80% polar heads were exposed to the external medium.

In conclusion, it is not surprising that the same results were obtained with cardiolipin-containing and phosphatidic acid containing vesicles: the state of ionization of these two phospholipids may be the same at pH 7.4 in the presence of positive ligands, and their distribution between the leaflets of the bilayers is the same.

Taking these results into account, we can infer that about 2 mol of Adr per EPA can be accommodated in site I. The constant of association (K_I) for this site is $\simeq 10^5$. One mole of Adr can be embedded per ~ 2.5 mol of EPA with $K_{II} \simeq 4 \times 10^9$. Comparable values were obtained for the interaction between Adr and CL-containing LUV. In contrast, only one molecule of Adr can be accommodated in site I of EPG-containing vesicles. Type II binding, that is, where the anthraquinone moiety is embedded in the membrane, was observed for low Adr to EPA molar ratios.

Our results compare well with those obtained by other methods. Adr binding to pure phosphatidylcholine in the gel state was found to be a weak (Karczmar & Tritton, 1979; Vilallonga & Philipps, 1978) or nonexistent (Goormaghtigh et al., 1980), depending on the absolute and relative concentrations of reactants used in the experiments. Adr binding to pure phosphatidylcholine in the liquid-crystalline state is a bit stronger (Karczmar & Tritton, 1979). The presence of negative charges strongly favors Adr binding (Duarte-Karim et al., 1976; Tritton et al., 1978; Karczmar & Tritton, 1979; Goormaghtigh et al., 1980). However, we did not observe the difference noted by these authors between cardiolipin and phosphatidic acid. The cause of this discrepancy may lie in the lipid media used: negatively charged SUV or LUV of EPC at 22 °C in our case; Folch medium (Duarte-Karim et al., 1976); negatively charged SUV of dipalmitoyl- or dimyristoylphosphatidylcholine near their phase transition temperatures (Tritton et al., 1978; Murphree et al., 1982); negatively charged phospholipid–dipalmitoylphosphatidylcholine monolayers at 25 °C (Goormaghtigh et al., 1980) in the other cases. Differences were also noted in the kinetics of interaction; the reaction took 10 s to be completed in our case and 100 min in the experiments with monolayers, thus confirming the importance of the medium used.

As for the location of the Adr molecule in the membrane, our conclusions are in partial agreement with those of Goldman et al. (1978) and Karczmar & Tritton (1979): the presence of small amounts of negative lipids in an EPC matrix creates two types of binding environment for the drug, one relatively exposed and the other more deeply buried in the membrane. Our results also indicate that the physical state of the lipid matrix is an important parameter for the penetration of the anthracycline moiety into the bilayer: in our case, as in the two former studies, the lipid matrix was in the liquid-crystalline state when such penetration occurred. A solid membrane tends to prevent the drug from penetrating deeply (Karczmar & Tritton, 1979). No penetration of the drug was observed with pure cardiolipin monolayers (Goormaghtigh et al., 1980). In this particular case, we observed a precipitation of pure CL SUV in the presence of Adr, which confirmed the observation of Nicolay et al. (1984) on pure CL liposomes.

Ionic strength appears to be an important factor since we observed that its increase diminishes the binding of Adr to negatively charged SUV, in agreement with the results of Karczmar & Tritton (1979). However, under conditions which closely resemble the physiological state, this binding is still sufficiently high to allow electrostatic interactions and therefore selective binding to CL-containing membranes.

ACKNOWLEDGMENTS

We are indebted to Laboratoire Roger Bellon for supplying us with adriamycin.

Registry No. Adr, 23214-92-8.

REFERENCES

Abramson, B. M., Katzman, R., Wilson, C. E., & Gregor, H. P. (1964) *J. Biol. Chem. 329*, 4066–4072.

Barthelemy-Clavey, V., Maurizot, J. C., Dimicoli, J. L., & Sicard, P. (1974) *FEBS Lett. 46*, 5–9.

Beraldo, H., Garnier-Suillerot, A., & Tosi, L. (1983) *Inorg. Chem. 22*, 4117–4124.

Blum, R. M., & Carter, S. K. (1974) *Ann. Int. Med. 80*, 249–259.

Bohren, C. F. (1976) *Chem. Phys. Lett. 40*, 391–394.

Chaires, J. B., Dattagupta, N., & Crothers, D. M. (1982) *Biochemistry 21*, 3927–3932.

Dahl, G., Azarnia, R., & Werner, R. (1981) *Nature (London) 289*, 683–685.

Davies, K. J. A., Doroshow, J. H., & Hochstein, P. (1983) *FEBS Lett. 153*, 227–230.

Di Marco, A. (1975) *Cancer Chemother. Rep., Part 1 6*, 91–95.

Doroshow, J. H. (1981) *J. Pharmacol. Exp. Ther. 218*, 206–211.

Duarte-Karim, M., Ruysschaert, J. M., & Hildebrand, J. (1976) *Biochem. Biophys. Res. Commun. 71*, 658–663.

Duvernay, V. H., Mong, S., & Crooke, S. T. (1980) in *Anthracyclines: Current Status and New Developments* (Crooke, S. T., & Reich, S. D., Eds.) Academic Press, New York.

Ferrans, V. J. (1978) *Cancer Treat. Rep. 62*, 955–961.

Fiallo, M. L., & Garnier-Suillerot, A. (1985) *Biochim. Biophys. Acta* (in press).

Forssen, E. A., & Tökés, Z. A. (1979) *Biochem. Biophys. Res. Commun. 91*, 1295–1301.

Forssen, E. A., & Tökés, Z. A. (1981) *Proc. Natl. Acad. Sci. U.S.A. 78*, 1873–1877.

Gabbay, E. J., Grier, D., Fingerle, R. E., Reiner, R., Levy, R., Pearce, S. W., & Wilson, W. D. (1976) *Biochemistry 15*, 2062–2070.

Gabizon, A., Dugan, A., Goren, D., Barenholz, Y., & Fuks, Z. (1982) *Cancer Res. 42*, 4734–4739.

Goldman, R., Facchinetti, T., Bach, D., Raz, A., & Shinitzki, M. (1978) *Biochim. Biophys. Acta 512*, 254–269.

Goodman, M. F., Lee, G. M., & Bachur, N. R. (1977) *J. Biol. Chem. 252*, 2670–2674.

Goormaghtigh, E., & Ruysschaert, J. M. (1984) *Biochim. Biophys. Acta 779*, 271–288.

Goormaghtigh, E., Chatelain, P., Caspers, J., & Ruysschaert, J. M. (1980) *Biochim. Biophys. Acta 597*, 1–14.

Israel, M., Modest, E. J., & Frei, E. (1975) *Cancer Res. 35*, 1365–1368.

Job, P. (1936) *Ann. Chim. 6*, 99–144.

Karcmzar, G. S., & Tritton, T. R. (1979) *Biochim. Biophys. Acta 557*, 306–319.
Lenaz, L., & Page, J. A. (1976) *Cancer Treat. Rep. 3*, 111–120.
Lentz, B. R., Madden, S., & Alford, D. M. (1982) *Biochemistry 21*, 6799–6807.
Leserman, L. D., Weinstein, J. N., Blumenthal, R., & Terry, W. D. (1980) *Proc. Natl. Acad. Sci. U.S.A. 77*, 4089–4090.
Malher, H. R. (1955) *Methods Enzymol. 2*, 688–693.
Martin, S. R. (1980) *Biopolymers 19*, 713–718.
Massari, S., Pascolini, D., & Gradenigo, G. (1978) *Biochemistry 17*, 4465–4469.
Murphee, S., Murphy, D., Sartorelli, A., & Tritton, T. (1982) *Biochim. Biophys. Acta 691*, 97–105.
Newman, G. C., & Huang, C. (1975) *Biochemistry 14*, 3363–3368.
Nicolay, K., Timmers, R. J. M., Spoelstra, E., Van der Neut, R., Fok, J. J., Huigen, Y. M., Verkleiy, A. J., & de Kruijff, B. (1984) *Biochim. Biophys. Acta 778*, 359–371.
Ptak, M., Egret-Charlier, M., Sanson, A., & Bouloussa, O. (1980) *Biochim. Biophys. Acta 600*, 387–397.
Rahman, A., Fumagalli, A., Goodman, A., & Schein, P. S. (1984) *Semin. Oncol. 11*, 45–55.
Ralston, E., Hjemeland, L. M., Klausner, R. D., Weinstein, J. N., & Blumenthal, R. (1981) *Biochim. Biophys. Acta 649*, 133–137.
Skovsgaard, T., & Nissen, N. I. (1982) *Pharmacol. Ther. 18*, 293–311.
Szoka, F., Olson, F., Heath, T., Vail, W., Mayhew, E., & Papahadjopoulos, D. (1980) *Biochim. Biophys. Acta 601*, 559–567.
Thayer, W. S. (1977) *Chem.-Biol. Interact. 19*, 265–278.
Tritton, T. R., & Yee, G. (1982) *Science (Washington, D.C.) 217*, 248–250.
Tritton, T., Murphree, S., & Sartorelli, A. (1978) *Biochem. Biophys. Res. Commun. 84*, 802–808.
Vilallonga, F. A., & Phillips, E. W. (1978) *J. Pharm. Sci. 67*, 773–775.
Wilschut, J., & Papahadjopoulos, D. (1979) *Nature (London) 281*, 690–692.
Zunino, F., Gambetta, R., Di Marco, A., & Zaccara, A. (1972) *Biochim. Biophys. Acta 277*, 489–498.

Diacylglycerols, Lysolecithin, or Hydrocarbons Markedly Alter the Bilayer to Hexagonal Phase Transition Temperature of Phosphatidylethanolamines†

Richard M. Epand
Department of Biochemistry, McMaster University, Health Sciences Centre, Hamilton, Ontario, Canada L8N 3Z5
Received March 14, 1985

ABSTRACT: The bilayer to hexagonal phase transition temperatures of dielaidoylphosphatidylethanolamine and 1-palmitoyl-2-oleoylphosphatidylethanolamine are 65.6 and 71.4 °C, respectively. Using high-sensitivity differential scanning calorimetry, I have shown that these transition temperatures are extremely sensitive to the presence of small amounts of other lipid components. For example, at a mole fraction of only 0.01, dilinolenin lowers the bilayer to hexagonal phase transition temperature of 1-palmitoyl-2-oleoylphosphatidylethanolamine by 8.5 °C. Other diacylglycerols have similar effects on this transition temperature, although the degree of unsaturation of the acyl chains has some effect, with distearin being less potent. In comparison, the 20-carbon alkane eicosane lowers this transition temperature by 5 °C, while palmitoyllysolecithin raises it by 2.5 °C. Similar effects of these additives on the bilayer to hexagonal phase transition temperature are observed with dielaidoylphosphatidylethanolamine. At these concentrations of additive, there is no effect on the gel-state to liquid-crystalline-state transition temperature. The observed shifts in the temperature of the bilayer to the hexagonal phase transition can be qualitatively interpreted in terms of the effects of these additives on the hydrophilic surface area and on the hydrophobic volume. Substances expanding the hydrophobic domain promote hexagonal phase formation and lower the bilayer to hexagonal phase transition temperature. The sensitivity of the bilayer to hexagonal phase transition temperature to the presence of additives is at least as great as that which has been observed for any other lipid phase transition.

Phospholipids in biological membranes are organized predominantly as bilayers although NMR studies have provided evidence for the presence of nonbilayer phases in sarcoplasmic reticulum vesicles (Davis & Inesi, 1971; Cullis & de Kruijff, 1979). A substantial fraction of the phospholipids which occur in biological membranes can readily be converted into a hexagonal phase when they are in pure form. Phosphatidylethanolamines containing an alkenyl ether bond in position 1 of glycerol undergo a bilayer to hexagonal phase transition close to physiological temperatures (Lohner et al., 1984). There is evidence that the formation of a hexagonal phase can have a marked effect on biological phenomena (Verkleij, 1984; Rilfors et al., 1984; Gordon-Kamm & Steponkus, 1984) including the functioning of the Ca^{2+}-ATPase of sarcoplasmic reticulum (Navarro et al., 1984). It is therefore of importance to determine the factors which modulate the bilayer to hexagonal phase transition. Using high-sensitivity differential scanning calorimetry, we can demonstrate that the temperature at which phosphatidylethanolamines undergo a bilayer to hexagonal phase transition is markedly sensitive to the presence of certain minor impurities.

† This investigation was supported by the Medical Research Council of Canada (Grant MT-7654).

0006-2960/85/0424-7092$01.50/0 © 1985 American Chemical Society